

Production of ceramic composite materials based on the ZrO_2 - Y_2O_3 - SiO_2 - TiB_2 system by the free SHS compression method

© Andrey P. Chizhikov^a✉, Alexander S. Konstantinov^a, Mikhail S. Antipov^a

^a Merzhanov Institute of Structural Macrokinetics and Materials Science Russian Academy of Science, 8, Academician Osipyan St., Chernogolovka, 142432, Russian Federation

✉ chij@ism.ac.ru

Abstract: The objective of this paper is to study the process of free SHS compression of composite materials in the ZrO_2 - Y_2O_3 - SiO_2 - TiB_2 system. The content of Y_2O_3 stabilizing additive varied in the ratio $(x-1)ZrO_2-xY_2O_3$ from 0 to 9 mol %. The influence of such technological parameters as the delay time, the strain rate, the pressing pressure, on the process of molding the selected materials, as well as the processes of phase and structure formation were studied. To establish the influence of the specified technological parameters on the process of selected materials molding, their formability was assessed. It was found that the nature of the dependences of the combustion characteristics of the studied materials on the content of the stabilizing additive correlates with the nature of the curves of the dependences of the degree of deformation on the delay time and the rate of deformation. It was shown that on the curve of the dependence of the degree of deformation on the pressing pressure, there is a limiting value, above which an increase in pressure does not affect the formability of the materials. It was shown that at a Y_2O_3 content of 0 to 4 mol %, the monoclinic and cubic modification of ZrO_2 is predominantly observed. A further increase in the Y_2O_3 content leads to the formation of a tetragonal modification of ZrO_2 in the obtained compact blanks. It was also found that in the studied materials the texture formation was observed in the direction perpendicular to the direction of pressure application.

Keywords: self-propagating high-temperature synthesis; free SHS compression; high-temperature deformation; zirconium oxide; yttrium oxide; composite material; titanium diboride; YSZ.

For citation: Chizhikov AP, Konstantinov AS, Antipov MS. Production of ceramic composite materials based on the ZrO_2 - Y_2O_3 - SiO_2 - TiB_2 system by the free SHS compression method. *Journal of Advanced Materials and Technologies*. 2025;10(3):190-199. DOI: 10.17277/jamt-2025-10-03-190-199

Получение керамических композиционных материалов на основе системы ZrO_2 - Y_2O_3 - SiO_2 - TiB_2 методом свободного СВС-сжатия

© А. П. Чижиков^a✉, А. С. Константинов^a, М. С. Антипов^a

^a Институт структурной макрокинетики и проблем материаловедения им. А. Г. Мерджанова РАН, ул. Академика Осипяна, 8, Черноголовка, 142432, Российская Федерация

✉ chij@ism.ac.ru

Аннотация: Настоящая работа посвящена изучению процесса свободного СВС-сжатия керамических композиционных материалов в системе ZrO_2 - Y_2O_3 - SiO_2 - TiB_2 . В качестве объекта исследования выбрана исходная порошковая система B_2O_3 - Zr - SiO_2 - Ti - B - Y_2O_3 . Содержание оксида иттрия, выступавшего в качестве стабилизирующей добавки, варьировалось в соотношении $(x-1)ZrO_2-xY_2O_3$ от 0 до 9 % моль. В работе изучено влияние таких технологических параметров свободного СВС-сжатия, как время задержки между иницированием реакции и приложением давления, скорость деформации, давление прессования на процесс формирования выбранных объектов исследования, а также процессы фазо- и структурообразования. Для установления влияния указанных технологических параметров на процесс формирования выбранных объектов исследования в работе проводилась оценка их формуемости. Установлено, что характер зависимостей характеристик горения исследованных материалов от содержания стабилизирующей добавки коррелирует с характером кривых

зависимостей степени деформации от времени задержки между инициированием реакции и приложением давления и скоростью деформирования. Показано, что на кривой зависимости степени деформации от давления прессования существует предельное значение, выше которого увеличение давления не оказывает влияния на формуемость материалов. Показано, что содержание Y_2O_3 от 0 до 4 % моль в полученных материалах преимущественно наблюдается моноклинная и кубическая модификация ZrO_2 . Дальнейшее увеличение содержания Y_2O_3 приводит к формированию тетрагональной модификации оксида циркония в полученных компактных заготовках. Также установлено, что в исследованных материалах после свободного СВС-сжатия наблюдалось образование текстуры в направлении, перпендикулярном направлению приложения давления.

Ключевые слова: самораспространяющийся высокотемпературный синтез; свободное СВС-сжатие; высокотемпературное деформирование; оксид циркония; оксид иттрия; композиционный материал; диборид титана; YSZ.

Для цитирования: Chizhikov AP, Konstantinov AS, Antipov MS. Production of ceramic composite materials based on the ZrO_2 - Y_2O_3 - SiO_2 - TiB_2 system by the free SHS compression method. *Journal of Advanced Materials and Technologies*. 2025;10(3):190-199. DOI: 10.17277/jamt-2025-10-03-190-199

1. Introduction

One of the urgent tasks of modern materials science is the development and creation of new materials with improved physical, mechanical and operational properties. One of the areas experiencing the need for such materials is the industry associated with high-temperature production, where materials are required that can operate under conditions of high thermal and mechanical loads [1–3]. To solve this problem, a promising solution is the use of composite materials based on zirconium dioxide [4, 5]. Due to its outstanding properties, such as high melting point, high hardness, fire resistance and chemical inertness, as well as a fairly low density [6], zirconium dioxide is the subject of a large number of research studies. In addition, by creating composite materials based on ZrO_2 , it is possible to improve its mechanical and operational properties. Today, a large number of different composite materials have been developed based on zirconium oxide with additives of aluminum oxide [7–9], magnesium oxide [10], silicon carbide [11], boron nitride [12, 13], molybdenum disilicide [14, 15], etc. It is known that the introduction of silicon oxide into a matrix based on ZrO_2 increases the refractory properties of the latter [16, 17]. In addition, the introduction of TiB_2 improves the tribological properties of materials based on zirconium dioxide [18, 19].

When making materials and products from zirconium dioxide-based ceramics, it is necessary to take into account that ZrO_2 undergoes a number of polymorphic transformations when heated [20, 21]. Namely, when heated to a temperature of 1170 °C, a transition from the monoclinic modification to the tetragonal one occurs, and when heated to 2370 °C, from the tetragonal to the cubic one. When cooling, the reverse transition occurs, and the monoclinic

modification is stable at room temperature. At the same time, the tetragonal modification is promising for high-temperature application. To prevent the transition from the tetragonal modification of ZrO_2 to the monoclinic one, various stabilizing additives are used. For example, CaO [22], MgO [23], CeO_2 [24], while Y_2O_3 is one of the most frequently used stabilizing additives [25].

Various methods are used to synthesize materials based on stabilized zirconium dioxide, including, the sol-gel method [26, 27], hydrothermal [28, 29], mechanochemical [30, 31], carbothermal synthesis [32], etc. To produce compact blanks, the materials produced by the listed methods are subsequently consolidated. For this purpose, sintering and various methods of force compaction are used, for example, hot isostatic pressing [33] or spark plasma sintering [34]. A common feature of this approach is a large number of technological operations, the need to use complex technological equipment, as well as high energy costs due to the need for long-term high-temperature processing. From this point of view, a combination of self-propagating high-temperature synthesis (SHS) [35] and subsequent high-temperature shear deformation is promising for obtaining composite materials based on stabilized ZrO_2 . Based on the specified combination, the free SHS compression method was developed [36–39]. Among the advantages of this method, it is possible to note the absence of complex technological equipment, the absence of the need to use external heating, and short process times. To date, compact blanks from various ceramic and metal-ceramic materials have been obtained using the free SHS compression method.

This paper seeks to investigate the effects of various process parameters in free SHS compression on the molding, phase, and structural formation

Table 1. Ratio of initial materials of the B₂O₃-Zr-SiO₂-Ti-B-Y₂O₃ composition

Composition No	Initial materials ratio, wt. %					Expected composition of synthesis products, wt. %					Y ₂ O ₃ content, mol %
	B ₂ O ₃	Zr	SiO ₂	Ti	B	Y ₂ O ₃	ZrO ₂	Y ₂ O ₃	SiO ₂	TiB ₂	
0	24.4	48.1	10.6	16.9	0	0	65	0	10.6	24.4	0
1	24.1	47.2	10.6	16.9	0	1.2	63.8	1.2	10.6	24.4	1
2	23.6	46.4	10.6	16.9	0.2	2.3	62.7	2.3	10.6	24.4	2
3	23.2	45.5	10.6	16.9	0.3	3.5	61.5	3.5	10.6	24.4	3
4	22.8	44.7	10.6	16.9	0.4	4.6	60.4	4.6	10.6	24.4	4
5	22.4	44	10.6	16.9	0.5	5.6	59.4	5.6	10.6	24.4	5
6	22	43.1	10.6	16.9	0.6	6.8	58.2	6.8	10.6	24.4	6
7	21.5	42.3	10.6	16.9	0.8	7.9	57.1	7.9	10.6	24.4	7
8	21.1	41.4	10.6	16.9	1	9	56	9	10.6	24.4	8
9	20.7	40.7	10.6	16.9	1.1	10	55	10	10.6	24.4	9

of ceramic plates derived from stabilized zirconium oxide materials. Specifically, we will examine the influence of delay time between the initiation of the reaction and the application of pressure, the rate of deformation, and the pressing pressure.

2. Materials and Methods

2.1. Initial materials and their ratio

The following powders were used as initial materials: boron oxide (> 99 %, < 2 μm), titanium (99.1 %, < 50 μm), silicon oxide (< 1 μm, > 99.3 %), zirconium (> 99 %, < 50 μm), boron (99.5 %, 10 μm), and yttrium oxide (99.95 %, < 10 μm). These powders were kept in a drying oven for 12 hours at a temperature of 50 °C to remove adsorbed moisture. Then, these raw materials were mixed in a ball mill for 12 hours in the ratios shown in Table 1.

2.2. SHS compression method

To study the dependencies of the process parameters of free SHS compression, the formability of the selected objects of study was assessed under conditions of a combination of SHS and high-temperature shear deformation processes. To conduct experiments to assess the formability, cylindrical blanks with a diameter of 30 mm and a height of 35 mm were prepared from the obtained mixtures of the initial reagents by the method of cold uniaxial pressing. The resulting blanks had a relative density of 0.65–0.70. These values of relative density correspond to the optimal range in which the maximum values of the combustion characteristics of the selected objects of study are realized. Then, the

resulting blanks were installed in a press; SHS was initiated by a tungsten spiral with a diameter of 1 mm, after which, after a certain delay time, external pressure was applied. Then, the degree of deformation Ψ was calculated for the deformed sample, which is taken as a criterion for the formability of the synthesized material. This value is expressed through the relative change in the cross section of the sample after deformation. The formula for calculating the degree of deformation is as follows:

$$\Psi = 1 - \frac{S_i}{S_f}$$

where S_i is cross-sectional area of the original sample before deformation, mm²; S_f is cross-sectional area of the synthesized material after deformation, mm².

Since the cross-section of the synthesized material after deformation is close to a circle, the average value is taken to calculate S_f :

$$S_f = \pi(d_{\max} + d_{\min})^2 / 16,$$

where d_{\max}, d_{\min} are maximum and minimum diameters of the synthesized material after deformation. The process diagram is shown in Fig. 1.

To study the influence of the combination of SHS and high-temperature shear deformation processes on the processes of phase and structure formation, compact ceramic materials based on the ZrO₂-Y₂O₃-SiO₂-TiB₂ system were obtained by the free SHS compression method. The scheme of the experiments on free SHS compression is shown in Fig. 2.

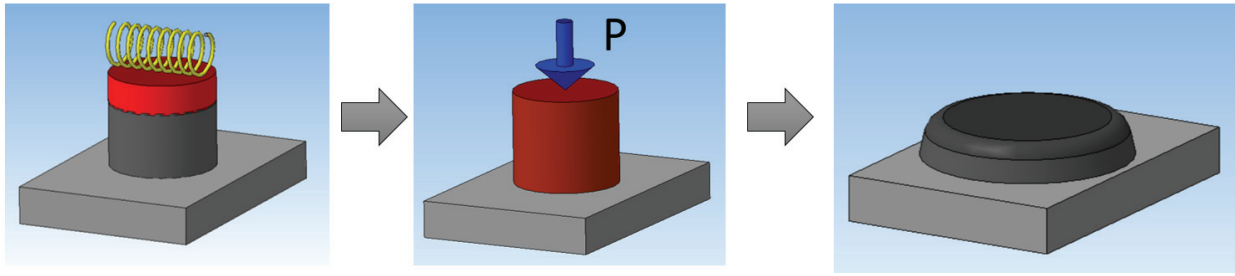


Fig. 1. Scheme of experiments to study formability

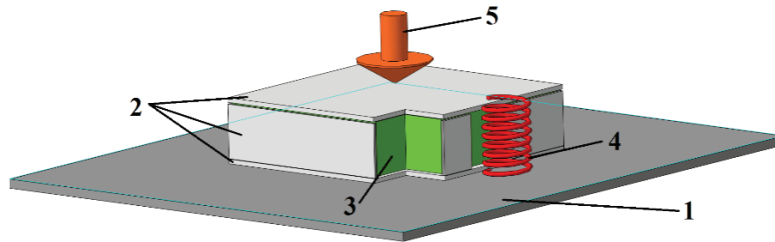


Fig. 2. Scheme of the free SHS compression process: 1 – substrate; 2 – asbestos insulation; 3 – original sample; 4 – tungsten spiral; 5 – direction of pressure application

The initial blank 3, made by cold uniaxial pressing, was installed on the metal substrate 1. The height was determined by the previously obtained value of the optimal relative density for each studied composition. The initial blanks were covered with thermal insulation 2 on each side. Synthesis was initiated by a tungsten spiral 4. After the combustion wave passed through the volume of the blank, after a certain delay time, external pressure was applied in the direction 5, perpendicular to the direction of front propagation.

2.3. Analytical methods

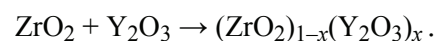
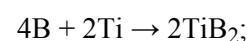
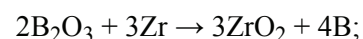
X-ray diffraction analysis (XRD) was performed on a DRON-3 diffractometer with a graphite monochromator on a secondary beam (CuK α radiation). The diffraction patterns were recorded in the step-by-step scanning mode in the angle range of $2\theta = 20\text{--}80^\circ$ with a step of 0.025° and an exposure of 4 s per point. The obtained diffraction patterns were analyzed using the ICDD PDF2 powder diffraction database (2022). The microstructure of the obtained materials was studied by scanning electron microscopy (SEM) using a Carl Zeiss LEO 1450 VP electron microscope.

3. Results and Discussion

3.1. Combustion characteristics in SHS mode

In this paper, a ceramic composite material based on yttrium oxide-stabilized zirconium oxide (YSZ) $\text{ZrO}_2\text{-Y}_2\text{O}_3\text{-SiO}_2\text{-TiB}_2$ was chosen as the

object of study was. The proportion of the stabilizing additive Y_2O_3 was from 0 to 9 mol %. The synthesis of materials in the SHS mode proceeded due to the reduction of boron oxide by zirconium with the formation of zirconium oxide and the release of free boron, which interacted with titanium to form titanium diboride. Silicon dioxide did not participate in the reaction in this case. When the stabilizing additive Y_2O_3 was introduced into the initial system, the total amount of oxygen increased. To reduce it, the proportion of boron oxide was reduced in compositions 1–9, which also led to a decrease in the amount of boron in the system. To compensate for this decrease, additional free boron was introduced into compositions 2–9. The use of boron oxide in this work is due to the fact that it is a cheap and readily available compound, the reduction reaction of which has a high thermal effect, which made it possible to obtain refractory zirconium oxide without significant energy costs. In addition, boron oxide is a cheap source of boron for the synthesis of titanium diboride. Below are the equations of the expected chemical reactions occurring during SHS:



It is also worth noting that, according to the XRD results, zirconium diboride phase was obtained in some samples. This means that part of the boron

was spent on interaction with zirconium and did not interact with titanium. At the same time, the reaction of ZrB_2 formation has a high thermal effect ($-76 \text{ kcal}\cdot\text{mol}^{-1}$), the value of which is close to the thermal effect of TiB_2 formation ($-70 \text{ kcal}\cdot\text{mol}^{-1}$). Thus, it can be assumed that the total thermal effect of the synthesis process did not change.

It was previously shown [69] that a change in the content of the stabilizing additive Y_2O_3 can affect the combustion characteristics of SHS systems. Thus, in the initial B_2O_3 -Zr-SiO₂-Ti system for the material without a stabilizing additive, the values of the temperature and combustion rate were $1808 \text{ }^\circ\text{C}$ and $5.1 \text{ mm}\cdot\text{s}^{-1}$, respectively. Further, with the introduction of Y_2O_3 , a monotonic increase in the temperature and combustion rate to values of $1836 \text{ }^\circ\text{C}$ and $8 \text{ mm}\cdot\text{s}^{-1}$ was observed at a Y_2O_3 content of 5 mol %. With a further increase in the Y_2O_3 content, a monotonic decrease in the combustion characteristics to $1784 \text{ }^\circ\text{C}$ and $5.1 \text{ mm}\cdot\text{s}^{-1}$ was observed at a Y_2O_3 content of 9 mol %. The dependences of the temperature and combustion rate of the studied materials on the Y_2O_3 content are shown in Fig. 3. Such behavior of the combustion characteristics can be explained by the fact that during the transition from the high-temperature tetragonal to the low-temperature monoclinic modification of ZrO_2 , a significant (up to 6 %) increase in volume is observed, the sample of composition 0 experiences more significant heat losses than the samples in which ZrO_2 is stabilized. Thus, increased heat losses lead to the fact that the samples of composition 0 have a lower combustion temperature than the samples with the addition of Y_2O_3 . According to the XRD results, zirconium diboride was observed in the synthesis products of

samples of compositions 0–4, while its amount monotonically decreased correlating with an increase in the combustion temperature of these samples. Zirconium diboride was not observed in the synthesis products of the sample of composition 5, thus the reaction of boron oxide reduction proceeded completely, and this sample had the highest combustion temperature. Further, with an increase in the Y_2O_3 content in the studied samples, a decrease in the combustion temperature was observed due to the dilution of the original system with yttrium oxide. The stabilizing additive Y_2O_3 was inert, did not participate in the reaction of product synthesis, but interacted with zirconium oxide to form a solid solution upon cooling.

3.2. High-temperature shear deformation of research objects

One of the important process parameters influencing the process of producing compact blanks by the free SHS compression method is the delay time. Ceramic materials are difficult to deform due to their mechanical properties and high melting point. Producing such materials in the SHS mode leads to the fact that the synthesis products are in a state heated to high temperatures (characteristic SHS temperatures are 1800 – $2500 \text{ }^\circ\text{C}$). As a result, ceramic materials acquire the ability to high-temperature deformation. In addition, the SHS process is not only the synthesis of materials in the combustion wave, but also the processes of phase and structure formation occurring behind the combustion front. This leads to the fact that for ceramic materials obtained in the SHS mode, there is an optimal temperature-time interval of processing, within which, under the action of high-temperature shear deformation, it is possible to obtain compact blanks with minimal porosity. When leaving this interval, structural defects and pores will form in the obtained samples. Thus, at small values of the delay time, due to the low completeness of the reaction of the initial components, the processes of phase and structure formation in the deformed samples may not be completed. In addition, since the characteristic temperatures of SHS often exceed the melting temperatures of most of the initial components, as well as some synthesis products, an excess amount of liquid phase may form in the deformed samples. The presence of a liquid phase has a positive effect on the ability of ceramic materials to high-temperature deformation. However, if there is an excess of it during deformation, the liquid phase will be squeezed out of the blank, causing deterioration of the phase composition, structure and an increase in

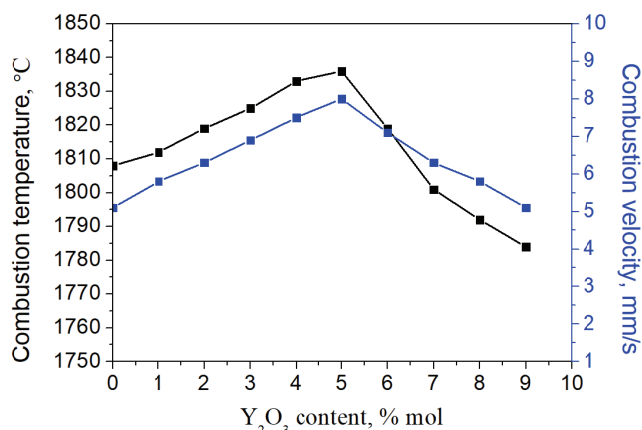


Fig. 3. Dependences of temperature and combustion rate of the studied materials on the Y_2O_3 content

porosity. If the delay time is excessive, the materials lose their ability to plastically deform due to cooling, which also leads to the occurrence of defects and cracks in the resulting blanks. Figure 4 shows the results of studying the effect of the delay time before applying pressure on the formability of the studied materials of compositions 0–9. As can be seen from Figure 4, for composition 0 without a stabilizing additive, the maximum value of the degree of deformation was 0.6. Further, with an increase in the proportion of Y_2O_3 , the maximum value of the degree of deformation monotonically increases to 0.75 (composition 5), after which it monotonically decreases to a value of 0.53 for composition 9. This type of dependence of the degree of deformation on the delay time correlates with the behavior of the dependences of the temperature and combustion rate on the proportion of Y_2O_3 , shown in Fig. 3. Namely, an increase in the content of yttrium oxide to 5 mol % leads to an increase in the combustion temperature and an improvement in the formability of the studied materials (compositions 0–5), and then to a decrease in both the combustion characteristics and the formability of the materials (compositions 6–9).

Figure 5 shows the curves of the dependences of the degree of deformation of the studied materials on the deformation rate. This process parameter has a significant effect on the production of compact ceramic blanks by the free SHS compression method. This effect is due to the fact that it was previously shown that SHS products containing a sufficient amount of liquid phase can have viscoelastic properties. Since the combustion temperature of the studied compositions exceeds the melting temperatures of the initial components (T_m of titanium is 1668 °C, T_m of boron oxide is 450 °C),

including silicon oxide (T_m is 1713 °C), which is an inert additive and is retained in the synthesis products, a sufficient amount of liquid phase is formed during SHS. As a result, the synthesis products are a solid-liquid suspension with viscoelastic properties, consisting of molten and partially unreacted initial components, as well as crystalline particles of the synthesis products. This leads to the fact that the viscosity of the synthesis products increases with the growth of the deformation rate. Thus, at high values of the deformation rate, due to the increase in the viscosity of the synthesized materials, the degree of deformation decreases, the formability of the materials worsens and macro and micro defects are formed. At low values of this parameter, the time of the SHS compression process increases, leading to cooling of the material, a decrease in its formability and the formation of defects.

As can be seen from Fig. 5, the dependence of the degree of deformation of the studied materials on the deformation rate also correlates with the dependences of the combustion characteristics shown in Fig. 3. With an increase in the proportion of the stabilizing additive and with an increase in the combustion temperature, the value of the deformation rate at which the maximum value of the degree of deformation is achieved decreases. The maximum value of the degree of deformation of 0.75 was obtained for composition 5 at the minimum value of the deformation rate among all the studied materials, namely $75 \text{ mm}\cdot\text{s}^{-1}$. This is due to the fact that composition 5 has the highest melting point, and, as a result, as a result of SHS of this composition, the largest amount of solid-liquid suspension is formed, the viscosity of which increases with an increase in the deformation rate.

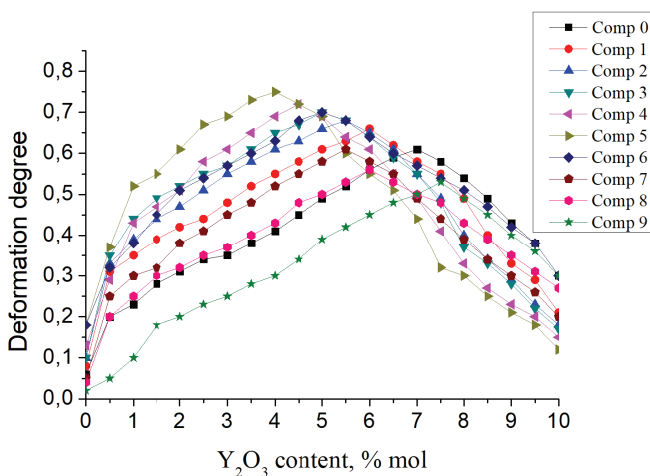


Fig. 4. Dependence of the degree of deformation of the materials under study on the delay time

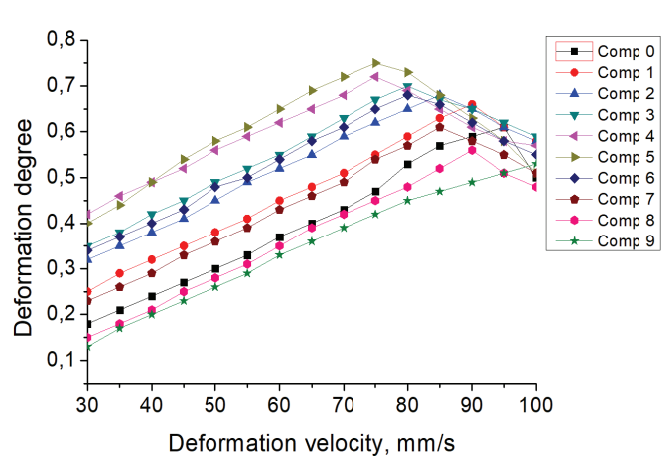


Fig. 5. Dependence of the degree of deformation of the materials under study on the deformation rate

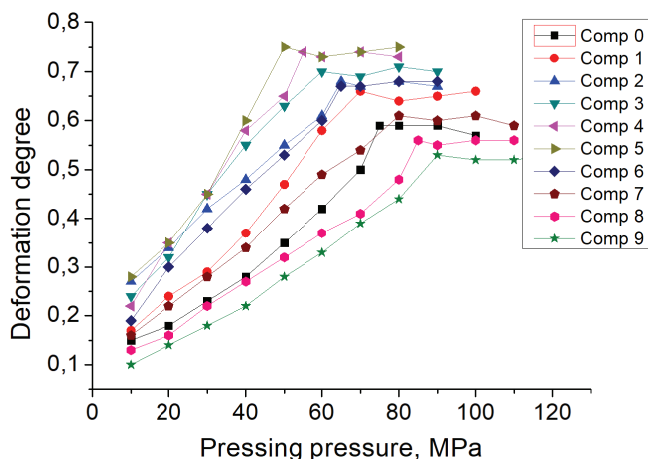


Fig. 6. Dependence of the degree of deformation of the materials under study on the value of pressing pressure

When studying the effect of pressing pressure on the process of molding ceramic blanks from the studied materials, it was found that there is a limiting value of this parameter, exceeding which does not further affect the molding process. Figure 6 shows the curves of the dependences of the degree of deformation of the studied materials on the pressing pressure. It is evident from the figure that the lowest value of pressing pressure required to achieve the maximum degree of deformation corresponds to composition 5 and is 50 MPa. Since this composition has the highest combustion temperature and, accordingly, has the greatest capacity for high-temperature deformation.

3.3. Phase composition and microstructure of the objects of study

When studying the effect of high-temperature shear deformation on the processes of phase and structure formation in the B_2O_3 -Zr-SiO₂-Ti-B-Y₂O₃ system, it was found that in materials 0–4 after deformation, the formation of four phases was observed, namely monoclinic and cubic zirconium dioxide, as well as titanium and zirconium borides, Fig. 7. At the same time, silicon dioxide, which is part of the initial reagents, is not displayed on the X-ray diffraction pattern, since it has an amorphous structure. However, the X-ray diffraction results do not show any compounds with silicon, thus, it can be concluded that silicon dioxide is retained in the synthesis products. At the same time, in similar materials obtained without applying pressure, the cubic modification of zirconium dioxide was absent, and tetragonal and monoclinic ZrO₂ were formed.

With increasing Y₂O₃ content in the starting materials (compositions 5–9), the samples obtained under free SHS compression conditions exhibited the formation of titanium diboride and tetragonal zirconium dioxide in the form of a solid solution (Zr_{0.875}Y_{0.125})O_{1.938} (ICDD PDF2 cardNo 10-81-8290). At the same time, in similar materials obtained without applying pressure, the formation of tetragonal ZrO₂ in the form of a solid solution (Zr_{0.75}Y_{0.25})O_{1.875} (ICDD PDF2 cardNo 10-81-8292) was observed.

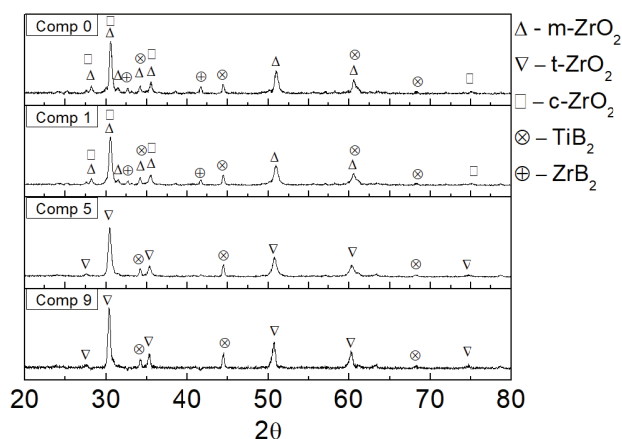


Fig. 7. Results of X-ray diffraction analysis of the materials under study produced by free SHS compression

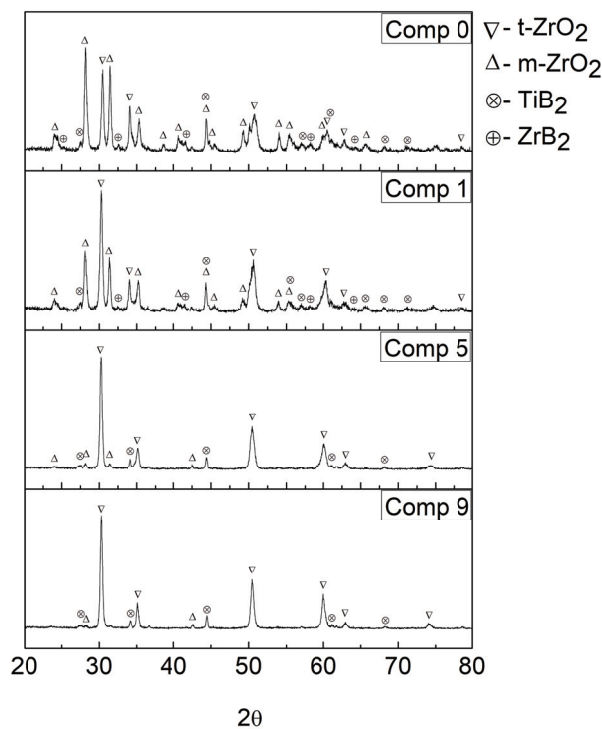


Fig. 8. SHS results of the produced materials without applying pressure

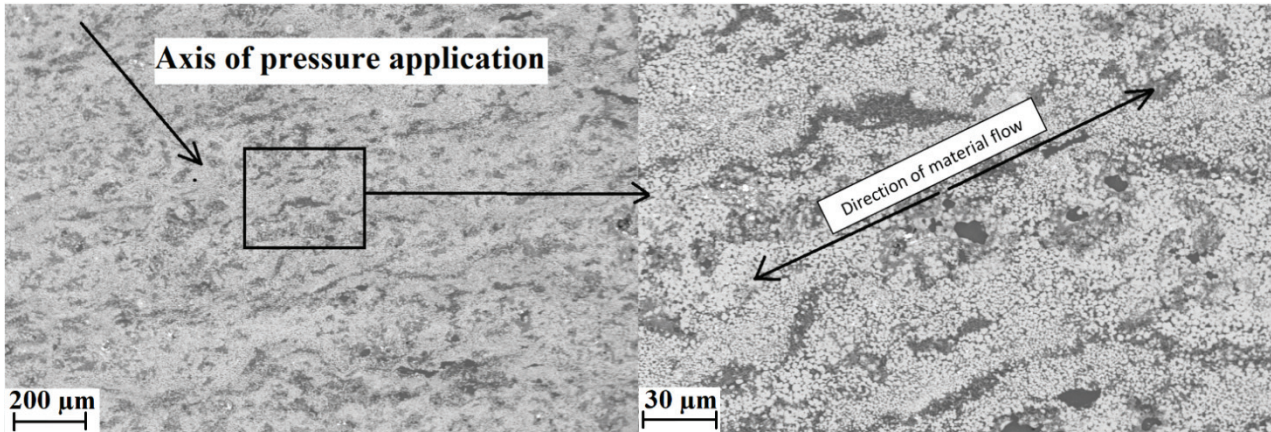


Fig. 9. SEM-images of the material based on composition 5 produced by the free SHS compression method

As the SEM-images of the produced compact ceramic materials showed, the formation of texture was observed in the structure of the samples obtained by the free SHS compression method. As shown in Fig. 9, during high-temperature shear deformation, the material is deformed in the direction perpendicular to the axis of pressure application, which promotes the healing of pores and cracks that may arise due to the nonequilibrium nature of the synthesis of materials in the SHS mode, as well as the formation of the corresponding texture.

In addition, it was found that for materials obtained in the B_2O_3 -Zr-SiO₂-Ti-B-Y₂O₃ system, high-temperature shear deformation does not lead to a significant increase in particle size compared to materials obtained without applying pressure. Thus, the size of zirconium dioxide in materials obtained under free SHS compression conditions was 5–6 μm, while in materials obtained without applying pressure, the average particle size of ZrO₂ was 2–4.

4. Conclusion

Compact ceramic materials based on stabilized zirconium oxide in the initial B_2O_3 -Zr-SiO₂-Ti-B-Y₂O₃ powder system were produced using the free SHS compression method. The proportion of the stabilizing additive in the $(1-x)ZrO_2-xY_2O_3$ ratio was from 0 to 9 mol %. The influence of such process parameters of free SHS compression as the delay time between reaction initiation and pressure application, deformation rate, pressing pressure on the molding process, as well as on the processes of phase and structure formation of compact materials based on the above materials was studied. It was found that the dependences of the deformation degree of the studied materials on the delay time between reaction initiation and pressure application,

deformation rate and pressing pressure correlate with the dependences of the combustion characteristics of the studied materials on the Y₂O₃ content. The dependences of the deformation degree on the delay time of all the studied materials have a maximum, after which their ability to plastic deformation decreases. Thus, there is an optimal time interval for processing the studied materials by the free SHS compression method. It is shown that with an increase in the content of the stabilizing additive from 0 to 5 mol %, the maximum degree of deformation increases from 0.6 to 0.75. It was also found that an increase in the Y₂O₃ content to 5 mol % makes it possible to achieve the maximum value of the degree of deformation of 0.75 for the studied materials at a deformation rate of 75 mm·s⁻¹. An increase in the Y₂O₃ content makes it possible to achieve the maximum value of the degree of deformation for the studied materials at a minimum pressing pressure of 50 MPa. With a content of the stabilizing additive from 0 to 4 mol %, the obtained materials predominantly contain monoclinic and cubic modifications of ZrO₂. A further increase in the Y₂O₃ content leads to the formation of a tetragonal modification of zirconium oxide in the obtained compact blanks. It was also found that in the studied materials after free SHS compression, texture formation was observed in the direction perpendicular to the direction of pressure application.

5. Funding

The study was supported by a grant from the Russian Science Foundation No. 22-79-10182, <https://rscf.ru/project/22-79-10182/>

6. Conflict of interest

The authors declare no conflict of interest.

References

1. Shojaie-bahaabad M, Bozorg M, Najafizadeh M, Cavaliere P. Ultra high temperature ceramic coatings in thermal protection systems (TPS). *Ceramics International*. 2024;50(7):9937-9951. DOI:10.1016/j.ceramint.2023.12.372
2. Malinina EA, Myshletsov II, Buzanov GA, Kubasov AS, et al. A new approach to the synthesis of nanocrystalline cobalt boride in the course of the thermal decomposition of cobalt complexes $[\text{Co}(\text{DMF})_6]^{2+}$ with boron cluster anions. *Molecules*. 2023;28(1):453. DOI:10.3390/molecules28010453
3. Tang YT, Zhang Y, Wan L, Kuek N, et al. Architected superalloys: a pathway to lightweight high temperature materials. *Scripta Materialia*. 2025;260:116598. DOI:10.1016/j.scriptamat.2025.116598
4. Taurino R, Martinuzzi S, Padovano E, Caporali S, et al. Laser additive manufacturing of Al_2O_3 and ZrO_2 -based eutectic ceramic oxide: an overview. *Journal of the European Ceramic Society*. 2025;45(5):117133. DOI:10.1016/j.jeurceramsoc.2024.117133
5. Sivasankar MV, Chinta ML, Sreenivasa Rao P. Zirconia based composite scaffolds and their application in bone tissue engineering. *International Journal of Biological Macromolecules*. 2024;265:130558. DOI:10.1016/j.ijbiomac.2024.130558
6. Chitoria AK, Mir A, Shah MA. A review of ZrO_2 nanoparticles applications and recent advancements. *Ceramics International*. 2023;49(20):32343-32358. DOI:10.1016/j.ceramint.2023.06.296
7. Vakhshouri M, Talimian A, Najafzadehkhoe A, Gallardo-López Á, et al. Fabrication of Al_2O_3 - $\text{Y}_3\text{Al}_5\text{O}_{12}$ - ZrO_2 composites by single-step spark plasma sintering. *Journal of the European Ceramic Society*. 2025;45(10):117358. DOI:10.1016/j.jeurceramsoc.2025.117358
8. Kozerozhets IV, Panasyuk GP, Semenov EA, Voroshilov IL, et al. Mechanism of the conversion of γ - Al_2O_3 nanopowder into boehmite under hydrothermal conditions. *Inorganic Materials*. 2020;56(7):716-722. DOI:10.1134/S0020168520070092
9. Hao S, Su H, Zhao D, Li X, et al. Complex shaped Al_2O_3 /YAG/ ZrO_2 eutectic ceramics with excellent high temperature mechanical properties printed by vat photopolymerization. *Additive Manufacturing*. 2025;101:104703. DOI:10.1016/j.addma.2025.104703
10. Song Q, Zha X, Gao M, Shi J, et al. Influence of ZrO_2 on the phase composition and mechano-physical properties of MgO - ZrO_2 refractories prepared by cold isostatic pressing. *Ceramics International*. 2024;50(17):30474-30482. DOI:10.1016/j.ceramint.2024.05.345
11. Lu N, Meng Q, Hou X, Sun G, et al. Innovative fabrication and absorption enhancement in MgO -stabilized ZrO_2 /graphene composites. *Advanced Powder Technology*. 2025;36(1):104731. DOI:10.1016/j.apt.2024.104731
12. Bai W, Chen L, Wei B, Li K, et al. The effect of particle size gradation on the microstructure, mechanical and thermal physical properties of BN - ZrO_2 - SiC composites. *Journal of Materials Research and Technology*. 2024;33:8091-8098. DOI:10.1016/j.jmrt.2024.11.154
13. Chen M, Fan B, Lei H, Song Z, et al. Rapid densification mechanism and properties of $\text{h-BN}/\text{ZrO}_2$ composites with oxide additives by spark plasma sintering. *Journal of the European Ceramic Society*. 2023;43(13):5493-5502. DOI:10.1016/j.jeurceramsoc.2023.05.022
14. Zhu L, Ren X, Wang X, Kang X, et al. Microstructure and high-temperature oxidation resistance of MoSi_2 - ZrO_2 composite coatings for niobium substrate. *Journal of the European Ceramic Society*. 2021;41(2):1197-1210. DOI:10.1016/j.jeurceramsoc.2020.09.029
15. Quan C, Yang X, Luo J, Wang Z, et al. Preparation of $\text{MoSi}_2@/\text{ZrO}_2$ core-shell powders by hydrothermal-calcination and evaluation of low-temperature oxidation resistance. *Ceramics International*. 2023;49(8):12662-12671. DOI:10.1016/j.ceramint.2022.12.129
16. Yang X, Qing W, Feng C, Yin-Wei M, et al. Sol-gel process and high-temperature property of $\text{SiO}_2/\text{ZrO}_2$ - SiO_2 composites. *Ceramics International*. 2017;43(1):854-859. DOI:10.1016/j.ceramint.2016.10.020
17. Fu L, Wang B, Xia W. New insights into the formation mechanism of zircon in a ZrO_2 - SiO_2 nanocrystalline glass-ceramic: a TEM study. *Ceramics International*. 2022;48(18):27097-27105. DOI:10.1016/j.ceramint.2022.06.021
18. Xiong Z, Zhang K, Liao W, Liu T, et al. Laser powder bed fusion fabrication of TiB_2 -Modified Al_2O_3 - ZrO_2 eutectic ceramics: microstructure evolution and mechanical properties. *Ceramics International*. 2024;50(24):55577-55588. DOI:10.1016/j.ceramint.2024.10.418
19. Lv M, Chen W, Liu C. Fabrication and mechanical properties of $\text{TiB}_2/\text{ZrO}_2$ functionally graded ceramics. *International Journal of Refractory Metals and Hard Materials*. 2014;46:1-5. DOI:10.1016/j.ijrmhm.2014.04.019
20. Jithin PV, Dhamodaran A, Prajisha KP, Suman S, et al. Structural and optical properties of Ce-stabilized tetragonal phase and intense blue emission of monoclinic phase in ZrO_2 nanoparticles. *Journal of Luminescence*. 2025;277:120933. DOI:10.1016/j.jlumin.2024.120933
21. Shwailiya SA, Hameed MR. Multi-material functionally graded additive manufacturing of zirconia ceramic: a systematic review. *Open Ceramics*. 2025;21:100741. DOI:10.1016/j.oceram.2025.100741
22. Chen G, Ling Y, Li Q, Zheng H, et al. Stability properties and structural characteristics of CaO -partially stabilized zirconia ceramics synthesized from fused ZrO_2 by microwave sintering. *Ceramics International*. 2020;46(10):16842-16848. DOI:10.1016/j.ceramint.2020.03.261
23. Wen T, Yuan L, Yan Z, Jin Y, et al. Enhancement of the electrochemical performance in MgO stabilized ZrO_2 oxygen sensors by co-doping trivalent metal oxides. *Current Applied Physics*. 2022;39:133-139. DOI:10.1016/j.cap.2022.04.021
24. Li N, Yu N, Yi Z, An D, et al. CeO_2 -stabilised ZrO_2 nanoparticles with excellent sintering performances synthesized by sol-gel-flux method. *Journal of the European Ceramic Society*. 2022;42(4):1645-1655. DOI:10.1016/j.jeurceramsoc.2021.12.012

25. Caruso R, Mamana N. High pressure compaction and densification at 1200 °C of nano-sized ZrO₂-3 mol% Y₂O₃ powders obtained by sol-gel process. *Journal of Alloys and Compounds Communications*. 2025;6:100051. DOI:10.1016/j.jacomc.2024.100051
26. Rahmamehr E, Baghshahi S, Karami F. A comparative study on antibacterial properties of EuO, CuO, and ZnO doped ZrO₂ sol-gel coatings. *Ceramics International*. 2024;50(24):52205-52212. DOI:10.1016/j.ceramint.2024.07.364
27. Talukdar C, Pandey V, Husain MS, Kumar N, et al. Tuning of optical parameters of sol-gel synthesized ZrO₂ nanoparticles. *Optical Materials*. 2024;157:116349. DOI:10.1016/j.optmat.2024.116349
28. Marashdeh MW, Mahmoud KA, Alhindawy IG. Nano-engineered Fe-doped ZrO₂: A novel and sustainable gamma ray shielding material synthesized via a green hydrothermal approach. *Ceramics International*. 2025; 51(15):20270-20282. DOI:10.1016/j.ceramint.2025.02.192
29. Panasyuk GP, Kozerozhets IV, Danchevskaya MN, Ivakin YuD, et al. A new method for synthesis of fine crystalline magnesium aluminate spinel. *Doklady Chemistry*. 2019;487(2):218-220. DOI:10.1134/S0012500819080019
30. Zain M, Yasin KA, Haq S, Rehman W, et al. Effect of calcination temperature induced structural modifications on the photocatalytic efficacy of Fe₂O₃-ZrO₂ nanostructures: mechanochemical synthesis. *RSC Advances*. 2024;14(21):15085-15094. DOI:10.1039/D4RA01944J
31. Malinina EA, Goeva LV, Buzanov GA, Retivov VM, et al. Synthesis and thermal reduction of complexes [Ni_{Ln}][B₁₀H₁₀] (L = DMF, H₂O, n = 6; L = N₂H₄, n = 3): Formation of solid solutions Ni₃C_{1-x}B_x. *Russian Journal of Inorganic Chemistry*. 2020;65(1):126-132. DOI:10.1134/S0036023620010118
32. Irankhah R, Mobasherpour I, Alizadeh M, Moosavi Nezhad SM, et al. Carbothermal reduction of ZrSiO₄ for in situ formation of ZrO₂-based composites using spark plasma sintering. *Ceramics International*. 2023;49(2):2681-2688. DOI:10.1016/j.ceramint.2022.09.248
33. Li X, Xu Y, Mao X, Zhu Q, et al. Investigation of optical, mechanical, and thermal properties of ZrO₂-doped Y₂O₃ transparent ceramics fabricated by hip. *Ceramics International*. 2018;44(2):1362-1369. DOI:10.1016/j.ceramint.2017.08.204
34. Vakhshouri M, Najafzadehkhoe A, Talimian A, Pernia CL, et al. Al₂O₃/Y₃Al₅O₁₂ (YAG)/ZrO₂ composites by single-step powder synthesis and spark plasma sintering. *Journal of the European Ceramic Society*. 2024;44(12):7180-7188. DOI:10.1016/j.jeurceramsoc.2024.05.004
35. Lu N, He G, Yang Z, Yang X, et al. Fabrication and reaction mechanism of MgO-stabilized ZrO₂ powders by combustion synthesis. *Ceramics International*. 2022; 48(5):7261-7264. DOI:10.1016/j.ceramint.2021.11.286
36. Stolin AM, Bazhin PM, Alymov MI. Deformation of SHS products under combustion conditions. *Inorganic Materials*. 2016;52(6):618-624. DOI:10.1134/S0020168516060169
37. Bazhin P, Konstantinov A, Chizhikov A, Prokopets A, et al. Structure, physical and mechanical properties of TiB-40 wt.% Ti composite materials obtained by unrestricted SHS compression. *Materials Today Communications*. 2020;25:101484. DOI:10.1016/j.mtcomm.2020.101484
38. Stolin AM, Bazhin PM, Konstantinov AS, Stolin PA, et al. Free SHS-compression method for producing large-sized plates from ceramic materials. *Refractories and Industrial Ceramics*. 2019;60(3):261-263. DOI:10.1007/s11148-019-00348-4
39. Chizhikov AP, Konstantinov AS, Antipov MS, Zhidovich AS, et al. Self-propagating high-temperature synthesis of composite material based on stabilized zirconium oxide. *Refractories and Industrial Ceramics*. 2023;64(4):373-377. DOI:10.1007/s11148-024-00855-z

Information about the authors / Информация об авторах

Andrey P. Chizhikov, Cand. Sc. (Eng.), Senior Researcher, Merzhanov Institute of Structural Macrokinetics and Materials Science RAS (ISMAN), Chernogolovka, Russian Federation; ORCID 0000-0003-2793-6952; e-mail: chij@ism.ac.ru

Alexander S. Konstantinov, Cand. Sc. (Eng.), Researcher, ISMAN, Chernogolovka, Russian Federation; ORCID 0000-0002-0524-6283; e-mail: konstanta@ism.ac.ru

Mikhail S. Antipov, Junior Research, ISMAN, Chernogolovka, Russian Federation; ORCID 0000-0002-7498-428X; e-mail: m_antipov@ism.ac.ru

Чижиков Андрей Павлович, кандидат технических наук, старший научный сотрудник, Институт структурной макрокинетики и проблем материаловедения им. А. Г. Мержанова РАН (ИСМАН), Черноголовка, Российская Федерация; ORCID 0000-0003-2793-6952; e-mail: chij@ism.ac.ru

Константинов Александр Сергеевич, кандидат технических наук, научный сотрудник, ИСМАН, Черноголовка, Российская Федерация; ORCID 0000-0002-0524-6283; e-mail: konstanta@ism.ac.ru

Антипов Михаил Сергеевич, младший научный сотрудник, ИСМАН, Черноголовка, Российская Федерация; ORCID 0000-0002-7498-428X; e-mail: m_antipov@ism.ac.ru

Received 21 March 2025; Revised 26 April 2025; Accepted 28 April 2025



Copyright: © Chizhikov AP, Konstantinov AS, Antipov MS, 2025. This article is an open access article distributed under the terms and conditions of the Creative Commons Attribution (CC BY) license (<https://creativecommons.org/licenses/by/4.0/>).